

Wind-powered water pumping system for corn plantations under the food estate program on Sumba Island, Indonesia

Amiral Aziz¹, Didik Rostyono¹, Toha Zaky¹, Nurry Widya Hesty¹, Ifanda¹, Khotimatul Fauziah¹,
Ridwan Budi Prasetyo², Rudi Purwo Wijayanto³, Ario Witjakso¹, Taurista Perdana Syawitri¹,
Agustina Putri Mayasari⁴

¹Research Center for Energy Conversion and Conservation, National Research and Innovation Agency, South Tangerang, Indonesia

²Research Center for Hydrodynamic Technology, National Research and Innovation Agency, Yogyakarta, Indonesia

³Directorate of Technology Transfer and Audit Systems, National Research and Innovation Agency, Jakarta, Indonesia

⁴BKPUK, National Research and Innovation Agency, South Tangerang, Indonesia

Article Info

Article history:

Received Dec 22, 2023

Revised Jul 10, 2024

Accepted Jul 17, 2024

Keywords:

Central Sumba Regency

Food estate

Levelized cost of energy

Water pumping

Wind turbine

ABSTRACT

The Food and Agriculture Organization (FAO) released a communiqué in March 2020 cautioning about the possibility of a worldwide food emergency due to coronavirus disease (COVID-19). As a response to the food shortages brought on by the COVID-19 outbreak, the authorities of Indonesia initiated a nationwide program aimed at improving the country's food supply known as the food estate (FE), which was later incorporated into national strategic programs. The climate and availability of surface water sources in this region make establishing an FE area in the Central Sumba Regency difficult. Sumba, on the other hand, possesses wind energy resources that can be transformed into electrical energy and used to pump underground water for agricultural purposes. A wind-powered water pump (WPW) is being developed in this study to provide water for maize plantations in the FE region in Central Sumba District, Indonesia. The study on the levelized cost of energy (LCOE) for water pumping indicates that the wind-powered system is more economically viable than the diesel-powered alternative. The LCOE for a WPW pumping system is 6,994 IDR/kWh, whereas the LCOE for a diesel-powered system is 16,667 IDR/kWh. The overall net present value of WPW and diesel-powered systems is 708,667,200 IDR and 2,158,349,000 IDR, respectively. This study contributes significantly to informed decision-making for enhancing the performance viability of the wind water pumping system for the food estate program in Indonesia.

This is an open access article under the [CC BY-SA](https://creativecommons.org/licenses/by-sa/4.0/) license.



Corresponding Author:

Amiral Aziz

Research Center for Energy Conversion and Conservation, National Research and Innovation Agency

South Tangerang 15314, Indonesia

Email: amiral.aziz@brin.go.id

1. INTRODUCTION

In response to the Food and Agriculture Organization's (FAO) 2020 warning of a potential global food crisis due to the COVID-19 pandemic, Indonesia established the food estate (FE) program as part of its National Strategic Programs [1], [2]. This initiative addresses the interconnection between pandemic threats and food security risks. Indonesia should focus more on enhancing agriculture intensification for limited farmland, encouraging young people to work in agriculture, and consolidating agriculture to boost farmers' incomes [3]. Improving distribution mechanisms was necessary to ensure equitable access to food and prevent hoarding by specific consumer groups, which can cause scarcity for others [4], [5]. The program is

positioned as a strategic solution to potential food shortages by emphasizing measurable efforts and incorporating sustainability considerations. Other important variables to consider are policy assistance and the ability of business-oriented farmers to identify market opportunities. Choosing different commodities can maximize the social, ecological, and economic advantages [6]. The Indonesian government has decided to roll out the FE program in numerous regions, including Kalimantan [7]–[9], Papua [10], Riau [11], South Sumatra [10], North Sumatra [12], [13], and East Nusa Tenggara [14].

Central Sumba Regency, East Nusa Tenggara, one of the areas selected as the FE program area [14], was established in February 2021 on 11,000 hectares, consisting of 5,400 hectares of rice and 5,600 hectares of corn and other crops. The success of the program has prompted the local authority to consider further expansion to encompass 20,000 hectares. To ensure water security for the FE program, authorities implemented a plan for dams, water catchment, irrigation, and sustainable groundwater management [15]. Accurate irrigation water demand prediction is crucial for effective water resource management and optimal system design, especially during droughts when insufficient water supply can significantly impact crop yields. The optimal crop water requirement mainly depends upon the accurate estimation of evapotranspiration and crop coefficients [16], [17] and climate change [17]. The importance of considering crop-specific water requirements and irrigation methods has been highlighted by [18], [19]. Furthermore, the water requirements of several crops such as wheat, oat, carrot, and maize at different growth stages were estimated using non-weighing Lysimeters [20] and remote sensing technology has the potential to improve water management in maize agriculture [21]. Table 1 outlines the expected water requirements for maize plants, as per a proposal from the Ministry of Public Works of the Republic of Indonesia.

Table 1. Estimated water needs for corn plants from the Ministry of Public Works

Plant	Water needed (ton/ha)	Watering interval
Corn	Phase I: 9.5-13	Phase I: 2 twice/day (morning and noon)
	Phase II: 15-20	Phase II: Furrow irrigation (for generative phase)
	Phase III: 5-10	Phase III: 2 twice/day (morning and noon)
	Phase IV: 2-3.5	Phase IV: 3 times/3 days (noon) no Irrigation a week before harvest
	Phase I: 9.5-13	Phase I: 2 twice/day (morning and noon)

The conveyance of water between the water source and the irrigated land is the primary technique of providing water for irrigation. Water flow necessitates the expenditure of energy. The pumping plant comprises all the mechanical tools and equipment necessary to transport water from the source to the field. Important engineering difficulties are involved in the architecture, selection, installation, operation, and maintenance of the pumping plant. Various renewable energy-powered water pumping systems for agricultural applications have been investigated by researchers across the world [22]–[24]. Additionally, there has been a rapid decrease in the costs of renewable energy conversion technologies in the recent years [25], [26]. The use of hybrid renewable energy for water pumping (e.g., photovoltaic solar and wind) for agriculture is particularly advantageous because there are no operational greenhouse gases (GHG) emissions, which have been mainly attributed to climate change and have produced unprecedented consequences in recent times. The most popular renewable energy sources for water pumping applications are wind and solar. Wind turbines can gather energy from the wind [27]. The wind-powered water pumping (WPW) systems present a cost-effective, flexible, and secure water supply solution using clean energy [28]. Wind power decreases energy expenses to zero and saves on energy infrastructure expenditures wherever the application is put [28].

While existing research has explored WPW systems for agricultural applications, a knowledge gap exists regarding their design and implementation within the specific context of the FE program in Central Sumba, Indonesia. This study proposes a novel and potentially sustainable solution for water pumping in the FE program by developing a WPW system for corn crops. It conducts a comparative analysis of the economic viability of the WPW system against the conventional diesel-powered system, demonstrating the potential economic benefits of adopting wind energy for irrigation. The findings could contribute to informing policy decisions and promoting the adoption of renewable energy solutions for agricultural water management in Indonesia and other regions facing similar challenges.

2. METHOD

2.1. Site selection and pump system

The Central Sumba District has been chosen as an FE program area. It is located in the center of Sumba Island, 9°20'–9°50' S, 119°22'–119°55' E [29]. The pilot project of a 10-ha WPW pumping system was selected in the Central Sumba District of East Nusa Tenggara province of Indonesia, located on 9°24'24.952" S, 119°51'5.137" E. Figure 1(a) shows the wind speed map of Sumba Island [30]. Most of the

wind potential sites are located in the East Sumba District, and some are in the Central Sumba District. The wind speed in some areas, especially in the northern part and some in the Southeastern part of Sumba, can be more than 7.5 m/s. Figure 1(b) shows the wind speed map of Central Sumba District. There are some wind potential areas in the northern part, even though the wind speed in this district is slower than in the East Sumba District.

Figure 2(a) shows the slope map class 1 that indicates flat areas, and it can be interpreted as a plantation or rice field area. A slope map is a visual depiction of the inclination of a surface, providing insight into the degree of steepness or gentleness at specific locations. These maps are valuable tools for recognizing potential risks, devising construction initiatives, determining suitable locations for planting fields, and various other applications. The slope is the rise or fall of the ground surface. The wind speed potential map must be overlaid with the slope map to determine the probable placement of WPW pumping systems. Figure 2(b) depicts the intersection area between the slope map, and the wind speed map, denoted by gray-colored areas. These localities can be explored or chosen as locations for WPW pumping systems.

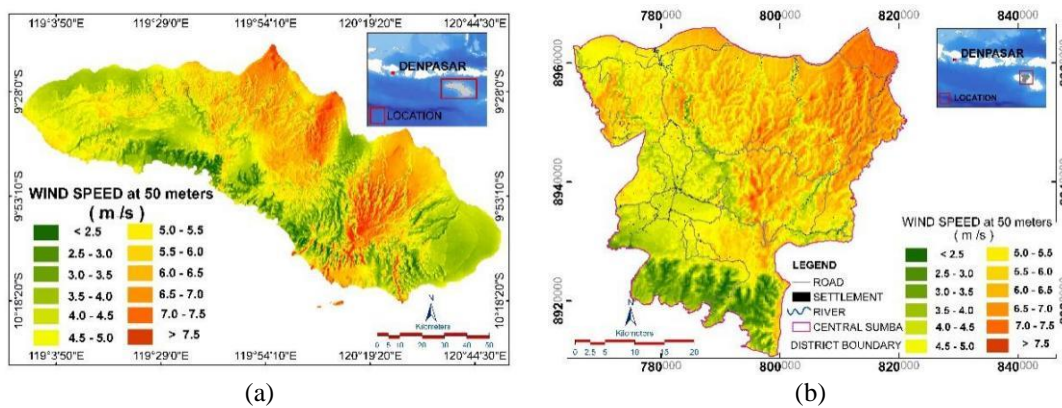


Figure 1. Wind speed map of (a) Sumba Island and (b) Central Sumba District

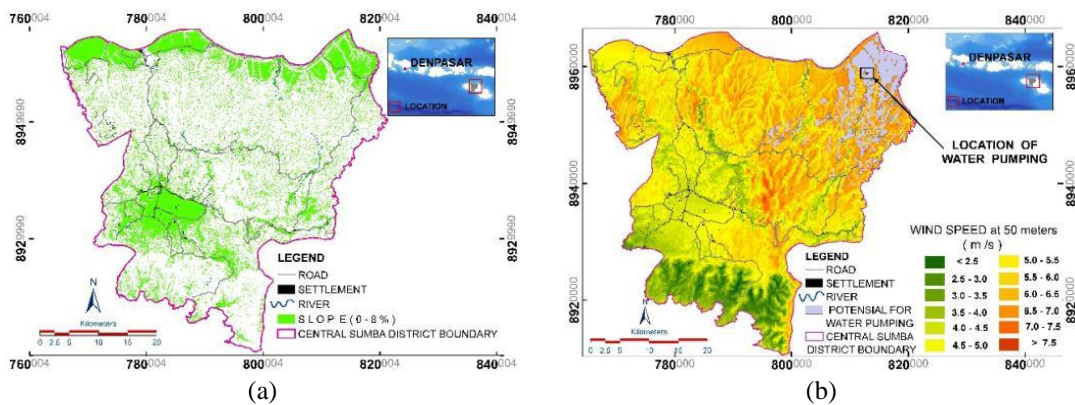


Figure 2. Map of Central Sumba District (a) slope map and (b) overlay of wind speed map and slope map

The land's economic value and suitability must be considered when selecting a location to develop corn plants. The slope was one of the dominant factors in this area that influenced the most suitable locations for corn production [31]. The exploitation land class shows that the highest level of farming efficiency is in the very suitable class 1 (S1) [32]. Based on these criteria, Figure 3(a) depicts the area to be piloted in this study, approximately 10 hectares in the northern section of the Central Sumba District. A wind turbine is installed at the highest point on the plantation's perimeter. The piping layout is shown in Figure 3(b). The four-inch-high density polyethylene (HDPE) pipe is used to deliver water from the pump to two water tanks. The pipe will end at a T-junction and branch out of the two tanks. The pipe that goes to the first tank (the farthest tank) from the junction point is 195 meters long horizontally with a diameter of 4 inches. After the horizontal pipe goes to the water tank tower, there is an elbow leading upwards so that there is a horizontal

pipe with the same diameter. Meanwhile, the pipe that goes to the second tank (nearest tank) from the junction point uses a polyvinyl chloride (PVC) pipe with a diameter of 3 inches and a length of 39 meters horizontally. On this line, there is a reducer to change the pipe diameter from 4 inches to 3 inches. This difference in pipes aims to get the same water discharge at the output end of the pipe. The submersible pump is built 20 meters underground and pumps water into two tanks within the plantation. The energy from the wind is extracted into electricity and stored in a battery bank, or it is directly used to pump underground water and store it in a storage tank. Wind energy water pumping systems use existing wind energy in the region to pump water to specific heights and store the pumped water.

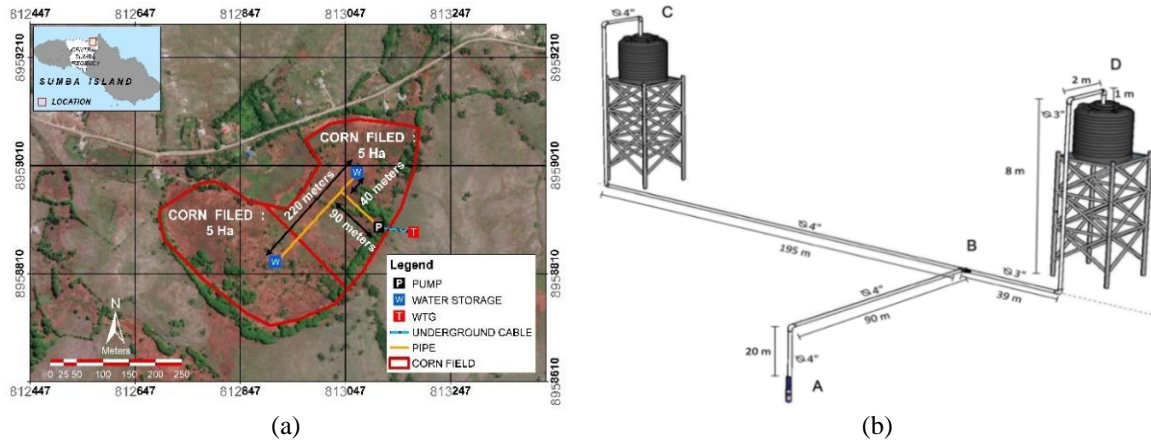


Figure 3. WPW pumping system (a) pilot location and (b) piping layout

2.2. Water pumping system sizing

2.2.1. Calculation of the total dynamic head

The total dynamic head of the pump (HP) can be calculated using the formula (1) [33], [34].

$$H_p = \frac{(p_d - p_s)}{\rho \times g} + H_s + H_d + H_f + \frac{(v_d^2 - v_s^2)}{2 \times g} \tag{1}$$

where p_d and p_s are discharge pressure and suction pressure, respectively, $p_d = p_s =$ atmosphere pressure, H_s and H_d are suction head and discharge head, respectively, and then H_f denotes the total pressure friction losses caused by the friction of the water as it flows through the pipeline. Total friction losses will be calculated by (2) for each length of straight pipe, filter, fittings, valve, bands, sudden contraction, and nozzle, where f is the friction constant, v is the velocity of water through the pipe, and g is gravity. The friction constant is affected by flow type (laminar or turbulent), pipe material, pipe roughness, and pipe diameter [28], [34], [35]. Friction losses through every length of straight pipe (H_{sp}) across the system were calculated using the Darcy-Weisbach formula in (3), where f is Darcy's friction constant, and D and L are the diameter and length of the pipe, respectively [34], [35]. K is the resistance coefficient of the filter, valve, fittings, bands, and sudden contraction [34], [35].

$$H_f = \sum H_{sp} + \sum K \times \frac{v^2}{2 \times g} \tag{2}$$

$$H_{sp} = f \times \frac{L}{D} \times \frac{v^2}{2 \times g} \tag{3}$$

The hydraulic power [36], [37] and total efficiency of the pump [34], [38] are respectively calculated by (4) and (5) where P_e is electric power input [39].

$$P_h = \rho \times g \times Q \times H_p \tag{4}$$

$$\eta_p = \frac{\rho \times g \times Q \times H_p}{P_e} \tag{5}$$

Figure 3(b) illustrates a pump supplying two branch lines that terminate at different elevations in an open-ended manner [34]. The approach in (6) to (9) are used to calculate total system resistance, total pump flow, and individual branch flows. Initially, it is noticed that i) the total flow must be equal to the sum of the branch flows; ii) the combined frictional resistance and elevation head for each branch, relative to junction 1, are the same [34], [35]; and iii) the flow divides to generate these identical total branch heads. As a result, the flow of each branch is added at multiple head points to generate curves CD. Supply line A is in series with branches C and D, and their system heads are algebraically combined for various flow conditions to obtain the total head. Let a main branch at B into two pipes of different sizes and different local features and let the elevation heads Z_C and Z_D at the end sections and the pressures p_C and p_D are the same as the atmospheric pressure.

$$\frac{p_B}{\rho \times g} = Z_C + \frac{p_{ATM}}{\rho \times g} + \sum h_{LOSSES} \quad (6)$$

$$\frac{p_B}{\rho \times g} = Z_C + \frac{p_{ATM}}{\rho \times g} + f_C \times \frac{L_C}{(D_C)^5} \times \frac{8 \times (Q_C)^2}{g \times \pi^2} + \sum K_C \times \frac{D_C}{(D_C)^5} \times \frac{8 \times (Q_C)^2}{g \times \pi^2} \quad (7)$$

$$\frac{p_B}{\rho \times g} = Z_D + \frac{p_{ATM}}{\rho \times g} + \sum h_{LOSSES} \quad (8)$$

$$\frac{p_B}{\rho \times g} = Z_D + \frac{p_{ATM}}{\rho \times g} + f_D \times \frac{L_D}{(D_D)^5} \times \frac{8 \times (Q_D)^2}{g \times \pi^2} + \sum K_D \times \frac{D_D}{(D_D)^5} \times \frac{8 \times (Q_D)^2}{g \times \pi^2} \quad (9)$$

Application of the continuity principle shows that the discharge in the main line is equal to the sum of the discharge in the branches. Thus, the following simultaneous equations may be written as (10) and (11),

$$Q_A = Q_C + Q_D \quad (10)$$

$$Q_C = Q_D = 0.5 \times Q_A \quad (11)$$

From (7) and (9), if $Z_C = Z_D$, it could be written in (1).

$$f_C \times \frac{L_C}{(D_C)^5} \times \frac{8 \times (Q_C)^2}{g \times \pi^2} + \sum K_C \times \frac{D_C}{(D_C)^5} \times \frac{8 \times (Q_C)^2}{g \times \pi^2} = f_D \times \frac{L_D}{(D_D)^5} \times \frac{8 \times (Q_D)^2}{g \times \pi^2} + \sum K_D \times \frac{D_D}{(D_D)^5} \times \frac{8 \times (Q_D)^2}{g \times \pi^2} \quad (12)$$

From (11), $Q_C = Q_D$, the (12) could be written in (13).

$$f_C \times \frac{L_C}{(D_C)^5} + \sum K_C \times \frac{D_C}{(D_C)^5} = f_D \times \frac{L_D}{(D_D)^5} + \sum K_D \times \frac{D_D}{(D_D)^5} \quad (13)$$

If f_C , L_C , $\sum K_C$, D_C , f_D , L_D , $\sum K_D$, Q_C , and Q_D are known, the diameter of pipe D (D_D) is determined by the iteration processes, as shown in Figure 4.

2.2.2. Calculation of the water tank

According to Table 1, the watering interval of corn plants is twice a day. Therefore, the size of the tank should be designed to be able to hold the water according to the corn plantation's needs. The formula for calculating the size of the water tank (WT) with the safety factor (S_F) considered can be expressed as (14).

$$S_F \times WT_{minimum} \leq WT \leq S_F \times WT_{maximum} \quad (14)$$

WT is the size of the water tank, S_F is the safety factor (in this case, 1.25, as it represents a 25% increase from the minimum, and the maximum water capacity), $\max WT$ is the maximum capacity of the water tank, and $\min WT$ is the minimum water that must be preserved for the corn plantation's needs. Using this formula, we can ensure that the water tank can accommodate the necessary water supply even in adverse conditions, as the safety factor accounts for potential contingencies like energy failure, additional water requirements, or water leakage.

2.2.3. Calculation of the wind turbine

A wind turbine is a device that converts the kinetic energy of the wind into electrical energy. The theoretical wind power production from wind flowing through the swept area A of a rotor during time t is shown in (15) [39], [40].

$$P_{WTG} = \frac{1}{2} \times \rho \times A \times v^3 \tag{15}$$

P_{WTG} , ρ , A , and v are the power output of the wind turbine in watts, air density in kg/m^3 , wind turbine rotor swept area in m^2 , and wind speed in m/s , respectively. However, wind speed exhibits randomness, volatility, and intermittent features, resulting in significant fluctuations in the output power of a wind turbine. Therefore, the formula (15) can be reformulated into (16).

$$P = \int_0^\infty P_{WTG} \times f(v) \times dv \tag{16}$$

where $f(v)$ is the probability density function of wind speed [41], [42]. The Weibull probability distribution has been widely used in wind analysis, planning, design, construction, and operation [30], [39].

$$f(v) = \frac{k}{c} \times \left(\frac{v}{c}\right)^{k-1} \times e^{-\left(\frac{v}{c}\right)^k}, k > 0; U > 0; C > 1 \tag{17}$$

The Weibull probability density function characterizing observed wind speed v (m/s) is denoted as $f(v)$ [39], [40]. The Weibull scale parameter, C , is defined in meters per second, while the dimensionless Weibull shape parameter is represented as k , typically falls between 1 and 3, delineating wind behavior by its velocity. Lower k values indicate variability in wind attributes, while higher k values signify relatively constant wind speeds.

2.3. Simulation procedure

The complete design process for the WPW pumping system for irrigation requires some basic steps to be taken: i) determine wind direction and resources, ii) calculate the water demand, iii) calculating the total dynamic head, iv) selecting a pump that will cover the electrical power requirements, v) wind turbine selection (sizing, number, and layout) to power the required pump electric load, vi) estimating wind energy production, and vii) estimating the levelized cost of energy [26], [27]. A simulation program is constructed based on the mathematical modelling of the system components and as per the algorithm shown in the flow chart presented in Figure 4.

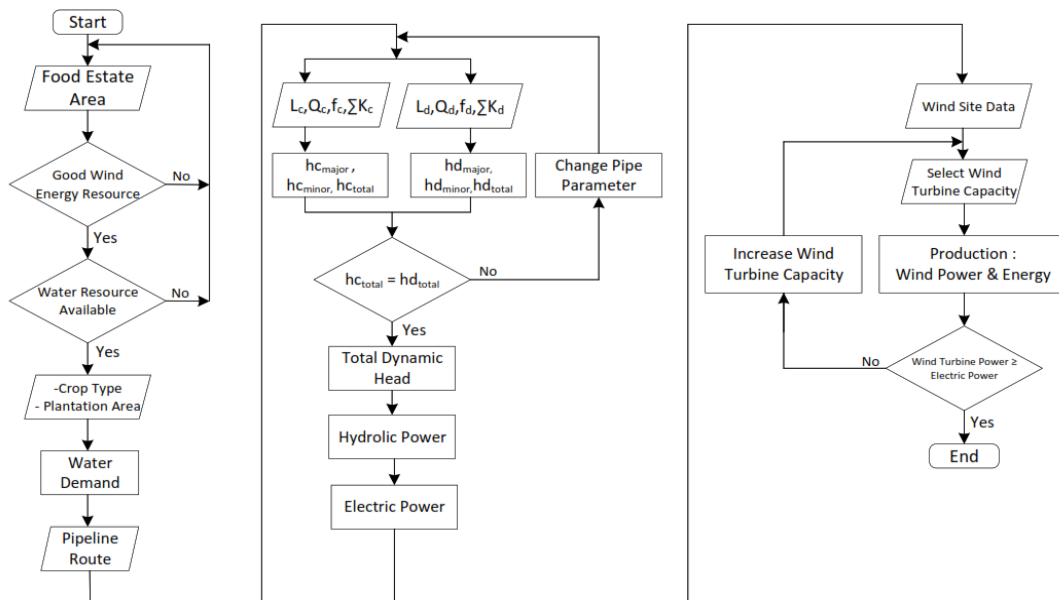


Figure 4. Flow chart of the present simulation model for a WPW pumping system design

3. RESULTS AND DISCUSSION

3.1. Design of the water pump system

The diameter of pipes BC and BD is determined using an iterative process as depicted in Figure 4. Once the pipe diameters BC and BD are obtained, minor losses and major losses can be calculated. Then the

total dynamic height of the pump can be calculated. If the capacity of each branch pipe is given, the hydraulic power of the pump can be calculated by using (4). The result of the iteration process for a 10-ha maize crop that uses 200 metric tons of water per day can be seen in Table 2. In Table 3, the WPW pumping system parameters and performance are shown. For a total head of 28.355 m and a capacity of 0.002894 m³/s, the hydraulic power and electric power are 804.869 W and 1073.872 W, respectively. The duration for filling the tank can be determined by considering the water requirements as listed in Table 2, the tank's capacity ensuring a desired level of safety, as indicated by (14), and the effectiveness of the pump engine's capacity. The findings, including the capacity of the tank and the time taken to fill the tank, are presented in Table 4.

Table 2. Characteristic of piping system

Pipe	D inside (m)	L (m)	Q (ton/day)	Q actual (m ³ /s)	D ⁵ (m ⁶)	f	ΣK	hf _{MAJOR} (m)	hf _{MINOR} (m)	h _{TOTAL} (m)
AB	0.0972	110	200	0.00289351	8.67624E-06	0.02	1.3	0.175273	0.01006	0.18534
BC	0.0972	206	100	0.00144675	8.67624E-06	0.02	0.9	0.082059	0.00174	0.08480
BD	0.0737	49.4	100	0.00144675	2.17439E-06	0.02	1.25	0.078520	0.00732	0.08584

Table 3. Parameter performance of WPW pumping system

Parameter	Unit	Value
Total dynamic head (H _p)	m	28.355
Capacity (Q)	m ³ /s	0.002894
Hydraulic power (P _{HYDRAULIC})	W	804.868
Pump efficiency		0.75
Electric power (P _{ELECTRIC})	W	1073.872

Table 4. Capacity of the water tank

Parameter	Unit	Value
Water requirements	ton/day	200
Water requirements with safety factor 1.25	ton/day	250
Conversion to L	m ³ /day	250
Optimum water tank capacity	m ³ /day	200
Tank capacity (in one time watering)	m ³	100
Pump capacity	m ³ /s	0,0029
Working assumption 80% of capacity	m ³ /s	0,0023
	m ³ /hour	8,33
Time to fill the tank	hours	12,00

3.2. Wind turbine selection

Since there is no wind measurement installed in the location, the global wind atlas data is used to assess the wind energy potential at the location. The time series graph in Figures 5(a) and (b) for the year 2021 shows the wind speed at two different heights, 30 meters (left, blue) and 50 meters (right, red). The peak wind speeds occur from May through September, while the lowest values are typically observed in November, December, and March.

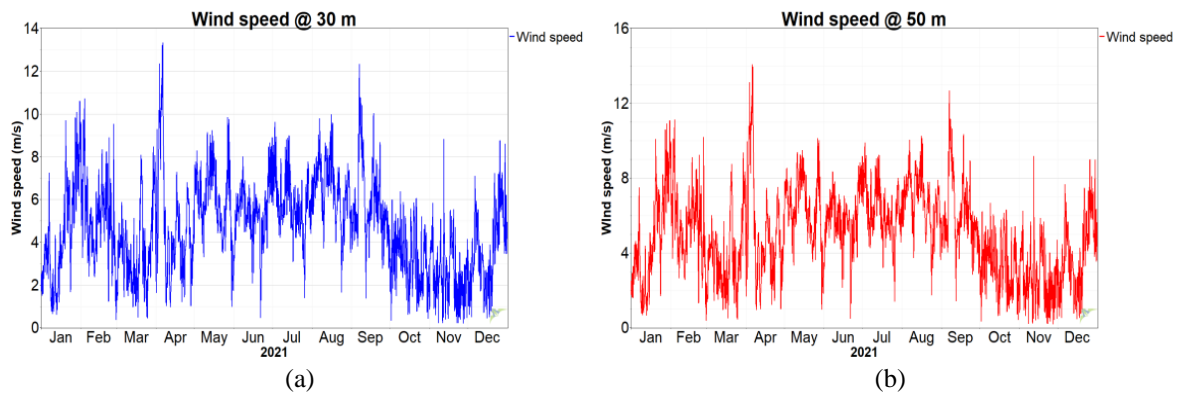


Figure 5. Wind speed at (a) 30 m and (b) 50 m

Figure 6 shows the Weibull parameter and the wind power density (WPD). The Weibull parameters $k = 2.37$ and $c = 5.68$ in wind speed distribution indicates that distribution is right-skewed with a wide range. It means that there are more days with high wind speeds than days with low wind speeds, and there is a chance of getting wind speeds that are higher and lower than the mean. The monthly Weibull parameters k is similar, ranging from 1.93 to 4.83, showing that the wind power distribution is right-skewed and consistent throughout the year. It means that there are more days with high wind power than days with low wind power and that the shape of the distribution is similar from month to month. The highest WPD occurs in August, with a value of 218 W/m^2 , while the lowest wind occurs in November, with 24 W/m^2 . On average, the location has a WPD of 127 W/m^2 .

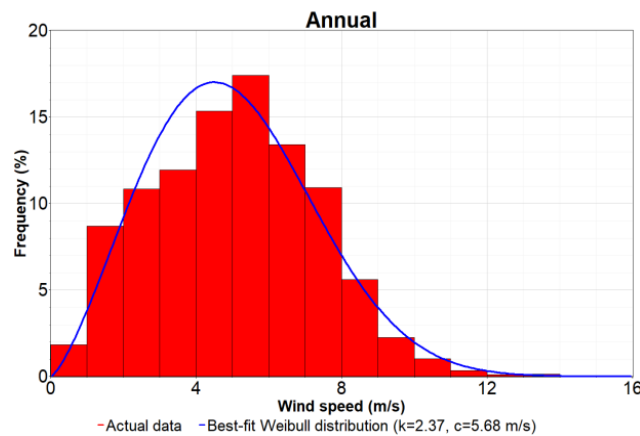


Figure 6. Weibull's distribution and WPD at 33 m

The wind rose diagram in Figure 7(a) shows that the prevailing wind direction at the location is from the southeast (SE). It means that the wind blows from the southwest (SW) more often than from any other direction. The wind also frequently blows from the west (W) and northwest (NW) relatively. The most common wind speeds are in the range of 4-8 m/s. However, the wind can also blow up to 12-16 m/s during the strong wind. From December through March, the dominant wind direction is from the NW. In April through November, the dominant wind direction is from the SE, consistent with the dry season. During the dry season, the prevailing winds come from the SE, known as the SE monsoon. These winds carry warm, moist air from the Australian continent and the Pacific Ocean towards Indonesia. As a result, the summer months in Indonesia are characterized by higher temperatures and increased humidity. The diurnal wind speed graph in Figure 7(b) shows that the average wind speed is generally higher in the afternoon than in the morning. It is likely due to the heating of the land surface during the day, which creates thermal updrafts that draw in cooler air from the surrounding area. The average wind speed also varies throughout the year, with higher average wind speeds in May through September and lower average wind speeds in October through April.

Figure 8 shows the power curves of the four selected turbines with data extracted from the producers' data-sheet for the following turbine models: the Endurance S-250, Enair 160, Bergey Excel-S 10 kW, and Proven 15 kW. It can be seen that the higher the rated power and cut-in speed, the more power the wind turbine can generate. The Endurance S-250 is a compact wind turbine with a rated power capacity of 5 kW. The power curve for the Endurance S-250 resembles a curve. It means that the Endurance S-250 produces more power at higher wind speeds. Meanwhile, the power curve for the Enair 160, the Bergey Excel-S 10 kW and Proven 15 kW have similar power curves. The Windographer software is used to simulate the capacity factor and energy production of some wind turbines ranging from 5 to 15 kW in order to meet the energy required by the water pumping system. Table 5 shows the monthly net capacity factor and net energy of wind turbines with varying capacities. The energy production of the 7.5 kW Enair 160 wind turbine is higher than the 10 kW Bergey Excell-S due to it is better power curve than the Bergey at the lowest wind speed ($<10 \text{ m/s}$).

Based on the data in Table 5, a 1.07-kW submersible pump load can be supplied by a 15 kW Proven wind turbine. The total energy production is about 35,637.88 kWh per year. Even though the capacity of a wind turbine is quite large compared to the pump load, the power output, especially in November, is quite small due to the low wind speed. For the rest of the months, the excess energy production is quite large, around 32,887 kWh/year. However, there is still an unmet load of around 2,045 kWh/year because of no wind at certain hours. The net capacity factor for all the wind turbines in this study is below 28%. It indicates

that the wind turbines are operating at a partial capacity for a significant portion of the time, suggesting that the wind turbines are not consistently generating electricity at their maximum potential, possibly due to wind speed fluctuations. Another tool (Homer) is used to simulate the energy production of a particular wind turbine at a certain location. The summary energy output of a 15 kW Proven wind turbine is shown in Table 6.

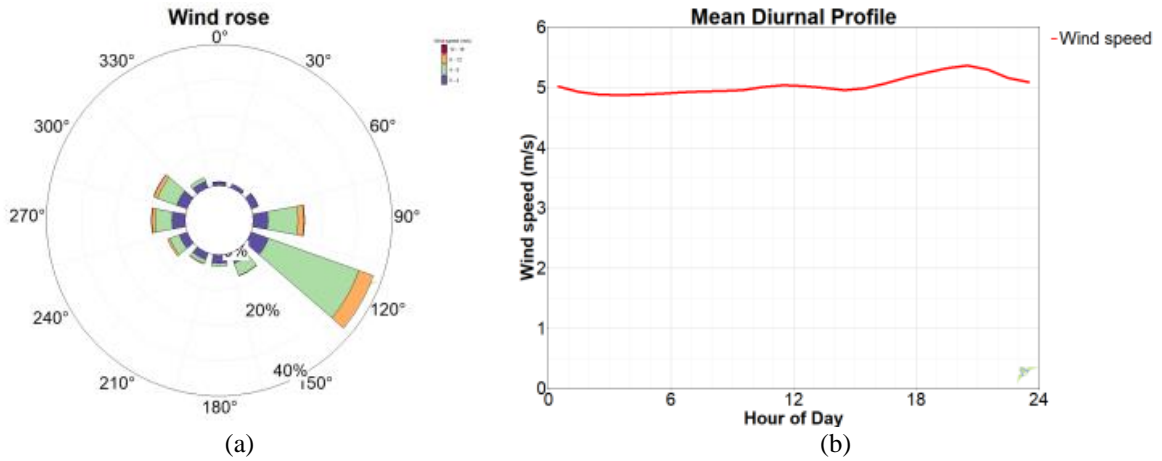


Figure 7. Profile of (a) wind rose and (b) mean diurnal

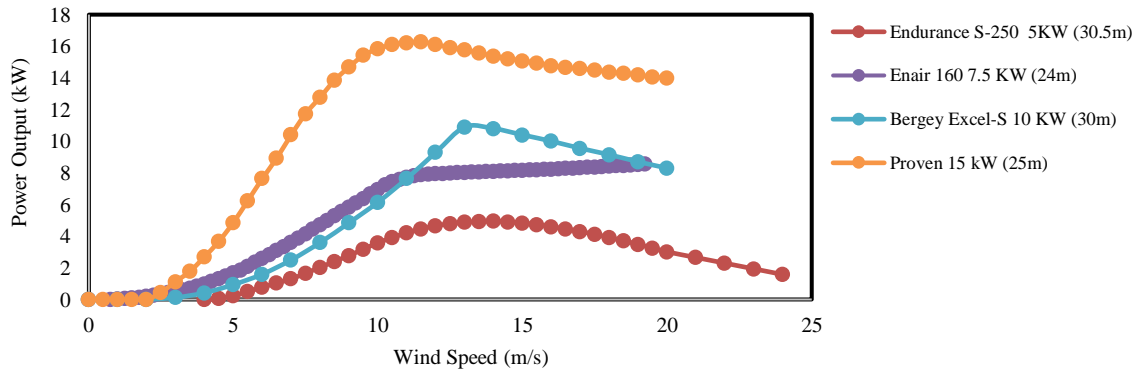


Figure 8. Power curve of wind turbines

Table 5. Monthly net capacity factor and net energy

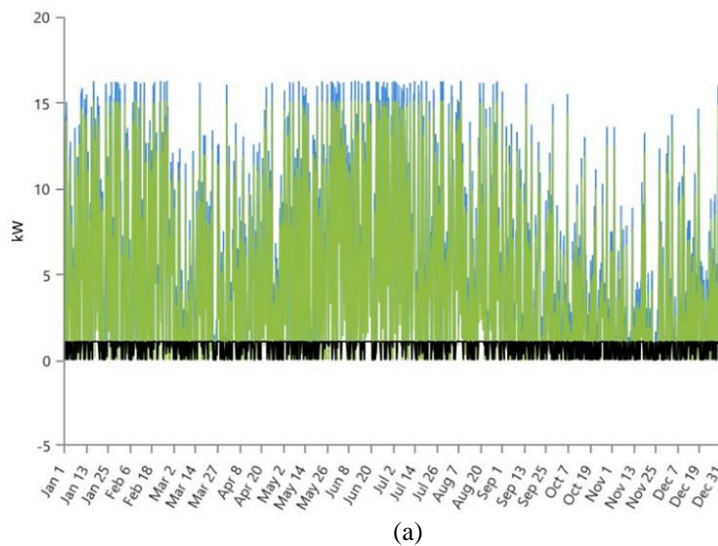
Month	Endurance S-250 5KW		Enair 160 7.5 KW (24m)		Bergey Excel-S 10 KW		Proven 15 kW (25m)	
	Net Capacity Factor (%)	Net Energy (kWh)	Net Capacity Factor (%)	Net Energy (kWh)	Net Capacity Factor (%)	Net Energy (kWh)	Net Capacity Factor	Net Energy (kWh)
Jan	8.87	329.84	17.74	989.99	9.3	691.72	23.9	2,667.47
Feb	10.02	336.82	21.66	1,091.85	11.21	753.31	30.26	3,050.53
Mar	3.42	127.13	10.57	589.87	4.58	340.83	13.83	154,397
Apr	10.94	393.74	20.26	1,093.94	11.93	858.68	25.54	2,758.82
May	15.31	569.64	28.55	1,592.86	15.58	1,159.09	40.75	4,547.54
Jun	9.81	353.11	22.6	1,220.65	11.36	817.64	32.93	3,555.96
Jul	13.67	508.56	27.3	1,523.42	14.43	1,073.26	39.2	4,374.34
Aug	19.13	711.6	34.03	1,898.63	18.66	1,388.66	48.14	5,372.45
Sep	14.57	524.36	28.33	1,529.80	15.42	1,110.04	38.99	4,211.01
Oct	1.09	40.68	8.06	449.99	2.79	207.35	10.2	1,138.74
Nov	0.65	23.31	5.28	285.04	1.67	120.41	5.95	642.38
Dec	3.9	144.92	11.76	655.97	5.19	386.31	15.9	1,774.66
Overall	9.28	4,063.71	19.67	12,922.01	10.17	8,907.29	27.12	35,637.88

Table 6. The summary of financial analysis in IDR (Indonesian Rupiah)

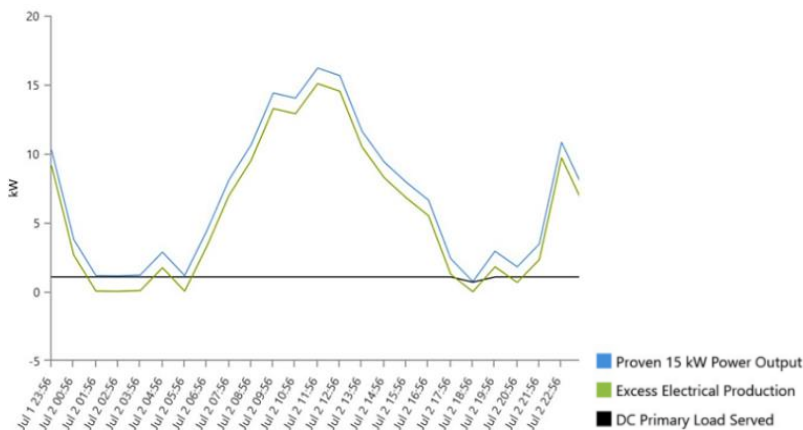
No	Item	Unit	15 kW Wind Turbine	2 kW Diesel Generator
1	Capital cost total:	IDR	222,000,000	75,300,000
	- Power generator	IDR	150,000,000	3,000,000
	- Rectifier, MPPT and Pump (lifetime 10 years)	IDR	46,900,000	47,300,000
	- Piping	IDR	25,000,000	25,000,000
2	Operation and maintenance cost (per year):	IDR	33,000,000	73,000,000
	- Fuel Oil	IDR	0	43,800,000 ^{*)}
	- Maintenance	IDR	33,000,000	30,000,000
	- Labor	IDR	30,000,000	30,000,000
3	Total net present cost	IDR	708,667,200	2,158,349,000
4	Levelized cost of energy	IDR/kWh	6,994	16,667
5	Lifetime	Year	20	20
6	Discount rate	%	8	8

^{*)} Fuel price 20,000 IDR/liter

The Homer software predicted the annual energy production of a 15 kW Proven wind turbine is around 40,629 kWh/year, higher than the prediction by Windographer software, i.e. 35,637.88 kWh/year. Since the load energy consumption is quite small (7,355 kWh/year), there is a substantial excess energy, around 32,887 kWh/year. This is due to Homer tried to meet the energy consumption in November even though the wind speed is quite low. Figure 9 illustrates how the Homer software predicts the performance parameters of a 15 kW wind turbine. Figure 9(a) shows the annual prediction of power output, excess power, and load, while Figure 9(b) shows the daily operation of performance prediction.



(a)



(b)

Figure 9. Power output, excess power and load served by a Proven 15 kW wind turbine (a) annually and (b) daily profile

3.3. Performance analysis of the wind-powered water pump system

The monthly water flow rates produced by various designed capacities of WPW pumping in Central Sumba are depicted in Figure 10. For each month, the water flow rate produced by the 15 kW wind turbine generator (WTG) is the highest of all WTG capacities. From Table 5, the highest WPD occurs in August at 218 W/m². The maximum flow rate for a 15 kW capacity wind turbine in August is 52.156 metric tons per month, while the other WTG is 13.481 metric tons per month, 18.432 metric tons per month, and 6.903 metric tons per month for turbines with capacities of 10 kW, 7.5 kW, and 5 kW, respectively. Even though the water flow rate produced by a WTG with a capacity of 5 kW is only 6.903 metric tons per month, the flow rate is still within the maximum capacity range of 7.5 tons per month and a minimum capacity of 5.625 tons per month. Only a WTG with a capacity of 15 kW can deliver a monthly water flow rate within the planned value range in November. Due to the low WPD of 24 W/m² in November, the WTG, with a capacity of 15 kW, produces only 6.236 tons of water each month, less than the maximum planned value. Despite being the lowest value of the 15 kW WTG, it can provide a water flow rate greater than the minimum permitted quantity. A wind turbine with a 5-kW capacity can generate water flow rates in the range of maximum and minimum values in August, while in other months, the 5 kW WTG produces water flow rates below the minimum value, so a WTG with a capacity of 5 kW does not meet the requirements to be selected in this study. Except in March, October, November, and December, a WTG with a capacity of 10 kW delivers a monthly water flow rate of more than 5.625 metric tons. Meanwhile, a WTG with a capacity of 7.5 kW delivers a monthly water flow rate greater than 5.625 metric tons except in March, October, and November.

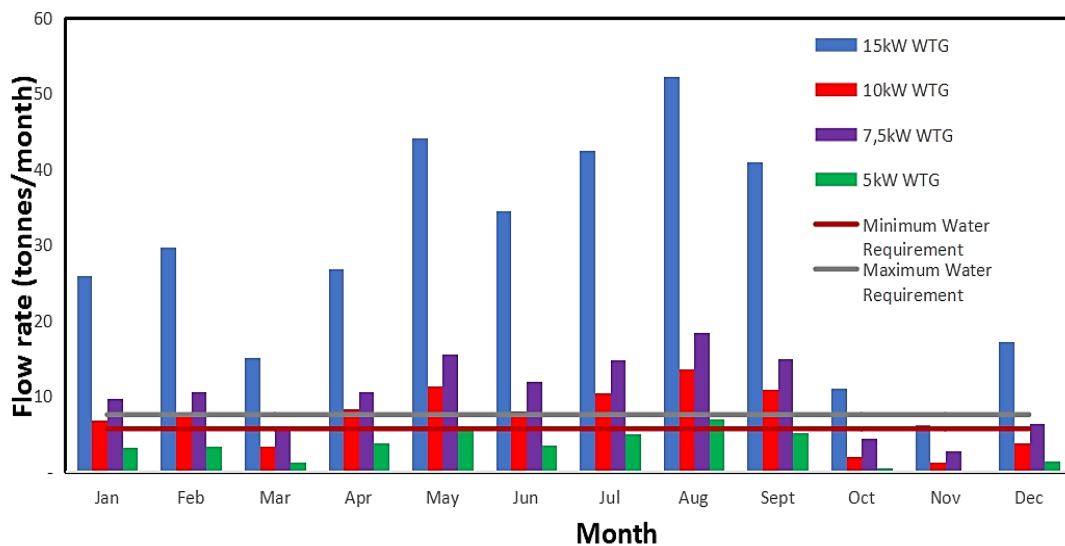


Figure 10. The monthly water flow rates are produced by various designed capacities of the wind-turbines

3.4. Levelized cost of energy analysis

To understand the feasibility of the wind-powered water pump (WPW) to be applied as water pumping system, this study compared the designed system with a diesel generator-powered water pumping system (DPW) as shown in Figure 11. The power supply of the water pumping system using a wind turbine is depicted in Figure 11(a), and Figure 11(b) shows the power supply of the water pumping system using a diesel generator. Table 6 highlights the financial analysis of a 15 kW wind turbine power and a 2-kW diesel generator power. Meanwhile, Figure 12 depicts the cash flow graphs for both water pumping systems: a wind turbine water pumping system, as shown in Figure 12(a) and a diesel generator water pumping system, as shown in Figure 12(b). It can be seen that a wind turbine has a higher initial investment than a diesel engine for the power source of water pumping system. However, the operational cost of a wind turbine is lower than that of a diesel engine. Hence, the optimum alternative is chosen based on the total present cost and the levelized cost of energy (LCOE) as shown in Table 7. It can be concluded that the WPW pumping system is the best option for watering the corn plantation compared to DPW system. This finding is in agreement with previous study by Girma *et al.* [36].

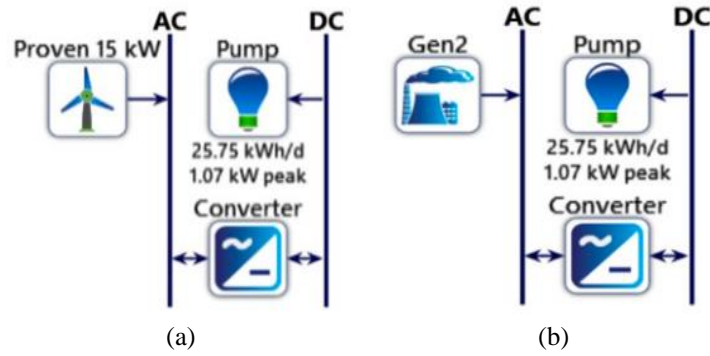


Figure 11. Power supply of water pumping system using (a) wind turbine and (b) diesel generator

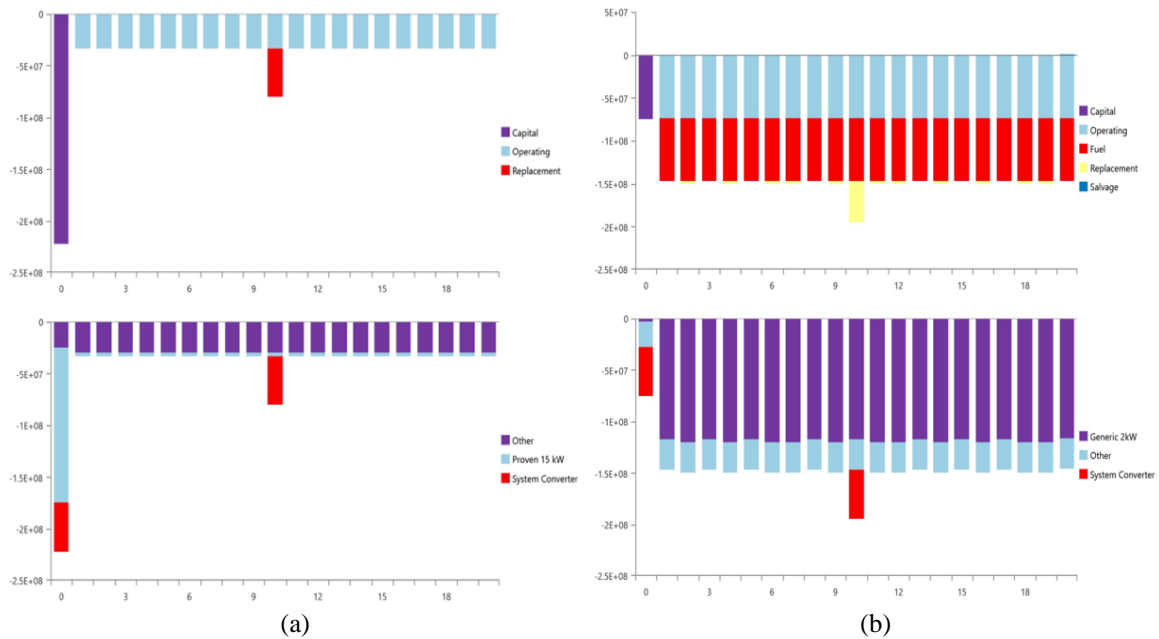


Figure 12. Cash flow of (a) WPW pumping system and (b) diesel-powered water pumping system

4. CONCLUSION

Due to the vast demand for sustainability, wind water pumping systems are seen as one of the feasible solutions for use in the food estate program in Central Sumba, Indonesia, where wind resources are available. The most common range of wind speeds in this area are 4–8 m/s. During the strong winds, the wind speeds can reach up to 12–16 m/s. The monthly water flow rate produced by various WPW pumping design capacities in Central Sumba indicates that only a 15 kW WTG is capable in producing a water flow rate greater than the minimum permitted limit of 5.625 metric tons per month. For the worst conditions due to low WPD of 24 W/m² in November, a WTG with a capacity of 15 kW is able to produce 6,236 tons of water per month, which is greater than the planned minimum value of 5,625 tons per month, so a WTG with a capacity of 15 kW is chosen in this research, and then a financial analysis is performed in comparison with diesel-powered water pumping system. The LCOE study found that that the wind-powered system is more economically viable than the diesel-powered alternative. The LCOE for a WPW pumping system is 6,994 IDR/kWh, whereas the LCOE for a diesel-powered system is 16,667 IDR/kWh. The overall net present value of wind-powered pumping systems and diesel-powered systems is 708,667,200 IDR and 2,158,349,000 IDR, respectively. This study contributes significantly in giving information about using wind energy as power source to the decision-maker. Therefore, the performance viability of the wind water pumping system of the FE program in Indonesia can be enhanced.

REFERENCES

- [1] Maskun, M. Napang, S. S. Nur, S. N. Bachril, and N. H. Al Mukarramah, "Detrimental impact of Indonesian food estate policy: conflict of norms, destruction of protected forest, and its implication to the climate change," *IOP Conference Series: Earth and Environmental Science*, vol. 824, no. 1, Jul. 2021, doi: 10.1088/1755-1315/824/1/012097.
- [2] D. Wisnu, "Food estate program law politics," *Journal of Contemporary Sociological Issues*, vol. 2, no. 1, Feb. 2022, doi: 10.19184/csi.v2i1.28051.
- [3] Z. Rozaki, "Food security challenges and opportunities in Indonesia post COVID-19," in *Advances in food security and sustainability*, 2021, pp. 119–168.
- [4] L. Lasminingrat and E. Efriza, "The development of national food estate: the Indonesian food crisis anticipation strategy," *Jurnal Pertahanan & Bela Negara*, vol. 10, no. 3, Dec. 2020, doi: 10.33172/jpbh.v10i3.1110.
- [5] D. Abdurrahman Miraj, U. Muthia Fathy, M. Nafik Hadi Ryandono, T. Sawarjuwono, S. Iswati, and A. Hendratmi, "Optimization of food estate program through cash waqf to achieve food sovereignty of Indonesia," *Proceedings of the 1st International Conference Postgraduate School Universitas Airlangga: "Implementation of Climate Change Agreement to Meet Sustainable Development Goals" (ICPSUAS 2017)*, 2018, doi: 10.2991/icpsuas-17.2018.65.
- [6] I. Yeny *et al.*, "Examining the socio-economic and natural resource risks of food estate development on peatlands: a strategy for economic recovery and natural resource sustainability," *Sustainability*, vol. 14, no. 7, Mar. 2022, doi: 10.3390/su14073961.
- [7] S. Marwanto and F. Pangestu, "Food estate program in Central Kalimantan Province as an integrated and sustainable solution for food security in Indonesia," *IOP Conference Series: Earth and Environmental Science*, vol. 794, no. 1, Jul. 2021, doi: 10.1088/1755-1315/794/1/012068.
- [8] I. Muhandiono and A. Hamdani, "Flood vulnerability impact for food estate potential in Central Kalimantan, Indonesia," *IOP Conference Series: Earth and Environmental Science*, vol. 648, no. 1, Feb. 2021, doi: 10.1088/1755-1315/648/1/012025.
- [9] N. Q. Hayati *et al.*, "Consumer preferences of vegetables and fruits at farmer's household level on the potential development of horticultural technology innovations in Central Kalimantan's food estate (case study in Village of Belanti Siam, District of Pandih Batu, Regency of Pulang Pisau, Central Kalimantan)," *IOP Conference Series: Earth and Environmental Science*, vol. 1153, no. 1, May 2023, doi: 10.1088/1755-1315/1153/1/012031.
- [10] A. A. Widiyanto, L. A. Perguna, M. N. Fatanti, M. Alam, and D. I. Perdana, "Food estate in transmigrant society, Central Borneo: blessed or curse?," *IOP Conference Series: Earth and Environmental Science*, vol. 1291, no. 1, Jan. 2024, doi: 10.1088/1755-1315/1291/1/012004.
- [11] R. Yulida, M. Ikhwan, Rosnita, and Y. Andriani, "Development strategy of program of model of sustainable food estate area (M-SFEA) based on female farmer group for social urban in Siak Regency of Riau Province, Indonesia," *IOP Conference Series: Earth and Environmental Science*, vol. 203, Dec. 2018, doi: 10.1088/1755-1315/203/1/012018.
- [12] D. Juhandi *et al.*, "Farm sustainability assessment and model: achieving food security through the food estate program in North Sumatra," *Land*, vol. 12, no. 10, Sep. 2023, doi: 10.3390/land12101833.
- [13] R. Sigalingging, J. Simanihuruk, N. S. Vinolina, and C. Sigalingging, "Analysis of energy used on shallot farming in food estate, Hutajulu, North Sumatra," *IOP Conference Series: Earth and Environmental Science*, vol. 1241, no. 1, Sep. 2023, doi: 10.1088/1755-1315/1241/1/012059.
- [14] Y. U. O. Sabaora, S. Heru Priyanto, and T. Mary Prihanti, "The food security of the household recipient of food independent village program in Central Sumba Regency," *SOCA: Jurnal Sosial, Ekonomi Pertanian*, vol. 15, no. 2, Jun. 2021, doi: 10.24843/SOCA.2021.v15.i02.p09.
- [15] ADB, "Policies to support investment requirements of Indonesia's Food and agriculture development during 2020-2045," *Asian Development Bank*, Manila, Philippines, Oct. 2019, doi: 10.22617/TCS190447-2.
- [16] M. L. Myint, "Evaluation of crop water requirements for Yazagyo irrigated area, Myanmar," *IOP Conference Series: Materials Science and Engineering*, vol. 849, no. 1, May 2020, doi: 10.1088/1757-899X/849/1/012090.
- [17] M. Le Page *et al.*, "Projection of irrigation water demand based on the simulation of synthetic crop coefficients and climate change," *Hydrology and Earth System Sciences*, vol. 25, no. 2, pp. 637–651, Feb. 2021, doi: 10.5194/hess-25-637-2021.
- [18] ADB, "Indonesia country water assessment," *Asian Development Bank*, <https://www.adb.org/documents/indonesia-country-water-assessment> (accessed Dec. 21, 2023).
- [19] T. Sun, Q. Huang, and J. Wang, "Estimation of irrigation water demand and economic returns of water in Zhangye Basin," *Water*, vol. 10, no. 1, Dec. 2017, doi: 10.3390/w10010019.
- [20] F. Hussain, M. A. Shahid, M. D. Majeed, S. Ali, and M. S. I. Zamir, "Estimation of the crop water requirements and crop coefficients of multiple crops in a semi-arid region by using Lysimeters," *Environmental Sciences Proceedings*, vol. 25, no. 1, doi: 10.3390/ECWS-7-14226.
- [21] S. H. Parmar, G. R. Patel, and M. K. Tiwari, "Assessment of crop water requirement of maize using remote sensing and GIS," *Smart Agricultural Technology*, vol. 4, Aug. 2023, doi: 10.1016/j.atech.2023.100186.
- [22] M. Al-Addous, S. Al Hmidan, M. Jaradat, E. Alasis, and N. Barbana, "Potential and feasibility study of hybrid wind-hydroelectric power system with water-pumping storage: Jordan as a case study," *Applied Sciences*, vol. 10, no. 9, May 2020, doi: 10.3390/app10093332.
- [23] M. Calero-Lara, R. López-Luque, and F. J. Casares, "Methodological advances in the design of photovoltaic irrigation," *Agronomy*, vol. 11, no. 11, Nov. 2021, doi: 10.3390/agronomy11112313.
- [24] J. M. Carricondo-Antón, M. A. Jiménez-Bello, J. M. Juárez, A. R. Tomas, and P. González-Altozano, "Optimization of an isolated photovoltaic water pumping system with technical-economic criteria in a water users association," *Irrigation Science*, vol. 41, no. 6, pp. 817–834, Nov. 2023, doi: 10.1007/s00271-023-00859-6.
- [25] Z. A. Khan, M. Imran, J. Umer, S. Ahmed, O. E. Diemuodeke, and A. O. Abdelatif, "Assessing crop water requirements and a case for renewable-energy-powered pumping system for wheat, cotton, and sorghum crops in Sudan," *Energies*, vol. 14, no. 23, Dec. 2021, doi: 10.3390/en14238133.
- [26] A. K. A. Zaher, E. Elgendy, M. Abdelhamid, and A. Mostafa, "Economic analysis of a solar operated irrigation pump for different crops under Egyptian climatic conditions," *International Journal of Renewable Energy Research*, 2023, doi: 10.20508/ijrer.v13i2.13956.g8731.
- [27] N. Argaw, R. Foster, and A. Ellis, "Renewable energy for water pumping applications in Rural Villages; period of performance: April 1, 2001--September 1, 2001," *Golden*, CO, Jul. 2003, doi: 10.2172/15004054.
- [28] Grundfos, "Irrigation pump handbook," *Grundfos*. (Accessed Dec. 22, 2023). [Online] Available: <https://api.grundfos.com/literature/Grundfosliterature-5840063.pdf>
- [29] Y. Ngongo *et al.*, "Land cover change and food security in Central Sumba: challenges and opportunities in the decentralization era

- in Indonesia,” *Land*, vol. 12, no. 5, May 2023, doi: 10.3390/land12051043.
- [30] Ifanda *et al.*, “Optimizing turbine siting and wind farm layout in Indonesia,” *International Journal of Renewable Energy Research*, 2023, doi: 10.20508/ijrer.v13i3.14070.g8806.
- [31] M. I. Habibie, R. Noguchi, M. Shusuke, and T. Ahamed, “Land suitability analysis for maize production in Indonesia using satellite remote sensing and GIS-based multicriteria decision support system,” *GeoJournal*, vol. 86, no. 2, pp. 777–807, Apr. 2021, doi: 10.1007/s10708-019-10091-5.
- [32] D. Maskumambang, B. Dipokusumo, and L. Sukardi, “Analysis of land suitability level and efficiency of corn farming business in Kempo District, Dompu,” *Jurnal Penelitian Pendidikan IPA*, vol. 7, no. SpecialIssue, pp. 351–358, Dec. 2021, doi: 10.29303/jppipa.v7iSpecialIssue.963.
- [33] “The handbook of technical irrigation information - a complete reference source for the professional,” *Hunter Industries*. https://www.hunterindustries.com/sites/default/files/tech_handbook_of_technical_irrigation_information.pdf (accessed Dec 22, 2023).
- [34] J. P. Messina, *General characteristics of pumping systems and system head curves*. Pump Handbook, 2001.
- [35] B. E. Larock, R. W. Jeppson, and G. Z. Watters, *Hydraulics of pipeline systems*. CRC Press, 1999.
- [36] M. Girma, M. Molina, and A. Assefa, “Feasibility study of a wind powered water pumping system for rural Ethiopia,” *AIMS Energy*, vol. 3, no. 4, pp. 851–868, 2015, doi: 10.3934/energy.2015.4.851.
- [37] Said M. A. Ibrahim, H. H. El-Ghetany, and A. G. M. Shabak, “Comprehensive design tool for sizing solar water pumping system in Egypt,” *Applied Solar Energy*, vol. 56, no. 1, pp. 18–29, Jan. 2020, doi: 10.3103/S0003701X20010053.
- [38] A. Sarr, A. Mérida-García, L. Diop, L. Mateos, N. Lamaddalena, and J. A. Rodríguez-Díaz, “Decision support tool for the optimal sizing of solar irrigation systems,” *Processes*, vol. 11, no. 3, Mar. 2023, doi: 10.3390/pr11030942.
- [39] S. Mathew, *Wind energy: fundamentals, resource analysis and economics*. Berlin, Heidelberg: Springer Berlin Heidelberg, 2006.
- [40] J. F. Manwell, J. G. McGowan, and A. L. Rogers, “Wind energy explained: theory, design and application,” John Wiley & Sons, 2010.
- [41] Y. Charabi and S. Abdul-Wahab, “Wind turbine performance analysis for energy cost minimization,” *Renewables: Wind, Water, and Solar*, vol. 7, no. 1, Dec. 2020, doi: 10.1186/s40807-020-00062-7.
- [42] J. Guillot, D. Restrepo Leal, C. Robles-Algarín, I. Oliveros, and P. A. Niño-Suárez, “Wind power prediction using a nonlinear autoregressive exogenous model network: the case of Santa Marta, Colombia,” *International Journal of Electrical and Computer Engineering*, vol. 13, no. 5, pp. 4856–4867, Oct. 2023, doi: 10.11591/ijece.v13i5.pp4856-4867.

BIOGRAPHIES OF AUTHORS



Amiral Aziz    received a B.Eng. degree in mechanical engineering from the National Institute of Science and Technology, Indonesia, in 1984 and an M.Sc. degree in thermal power and fluid engineering from the Victoria University of Manchester, UK, in 1991. Currently, he is a research professor at the Research Center for Energy Conversion and Conservation, National Research and Innovation Agency of the Republic of Indonesia (BRIN). His research interests include renewable energy, thermal power generation, hydroelectric power generation, auditing, and conservation of energy. He is also a lecturer at some universities in Indonesia. Furthermore, he can be contacted by email: amiral.aziz@brin.go.id or amiralaziz58@gmail.com.



Didik Rostyono    received a B.Sc. degree in electrical engineering from 10 Nopember Institute of Technology, Surabaya, in 1990, received a non-degree in grid connected wind energy converter in Deutsches Windenergie Institut GmbH, Germany in 1995 and received M.Sc. degree in electrical engineering from University of Indonesia in 1999. He is currently works as a researcher in renewable energy in the National Research and Innovation Agency (BRIN). He is also the chairman of the Wind Energy Technical Committee in the Indonesia National Standard (BSN), and as an observer member of the Wind Energy Technical Committee (TC88) in the International Electronically Commission (IEC). He can be contacted at email: didi007@brin.go.id or rostyono@gmail.com.



Toha Zaky    studied for a master's degree in electrical power systems at Bandung Institute of Technology, Indonesia. He currently serves as a Researcher at the Research Center for energy conversion and conservation within the National Research and Innovation Agency of The Republic of Indonesia (BRIN). Her research interests encompass the applications of renewable energy, electrical power system on renewable energy, and simulation optimization for renewable energy. For inquiries and collaborations, He can be reached via email at toha002@brin.go.id.



Nurry Widya Hesty    holds an M.Sc. degree in earth science from Bandung Institute of Technology, Indonesia. She currently serves as a researcher at the Research Center for Energy Conversion and Conservation within the National Research and Innovation Agency of The Republic of Indonesia (BRIN). Her research interests encompass the applications of renewable energy, geographic information systems (GIS), and mathematical modeling. For inquiries and collaborations, she can be reached at email: nurr010@brin.go.id or nurry.hesty@gmail.com.



Ifanda    received an M.Sc. degree in electrical engineering from Delft University of Technology, Netherlands, in 1994. Currently, he serves as a wind energy researcher at Research Center for Energy Conversion and Conservation – BRIN (National Research and Innovation Agency of The Republic of Indonesia) since 2019 and BPPT (The Agency for the Assessment and Application of Technology, 1994 – 2018). His research interests include the applications of renewable energy, Geography Information Systems. He can be contacted at email: ifanda@brin.go.id or ifanda64@gmail.com.



Khotimatul Fauziah    received a B.Eng. degree in electrical engineering from Institut Teknologi Sepuluh Nopember, Indonesia, in 2006 and M.Eng. degree in electrical and electronic engineering from Universitas Indonesia, Indonesia in 2014. She completed her Dr.Eng. degree from Shizuoka University, Japan in 2019. Currently, she is a researcher at the Research Center for Energy Conversion and Conservation, National Research, and Innovation Agency Republic of Indonesia. Her research interests include renewable energy technology, microgrid, nanoelectronics, and electric vehicle charging systems. She can be contacted at email: khot001@brin.go.id.



Ridwan Budi Prasetyo    received an M.Sc. degree in master of systems engineering from the University of Gajah Mada, Indonesia, in 2015. He has been a Research Center for Hydrodynamic Technology – National Research and Innovation Agency Republic of Indonesia (BRIN). He is currently a renewable energy in coastal areas researcher including wave energy and wind energy. He can be contacted by email at ridw007@brin.go.id.



Rudi Purwo Wijayanto    holds a PhD in mechanical science and engineering from Kanazawa University, Japan and also registered as an alumnus of Lund University, Sweden. He is currently a researcher at the National Research and Innovation Agency (BRIN). He is also a lecturer at Indonesian Institute of Technology (ITI) and Telkom University. He is interested in the renewable energy area including solar and wind turbines, energy conservation, energy audit, and technology transfer. He can be contacted by email: rudi014@brin.go.id.



Ario Witjakso    studied computer science at Nagaoka University, Japan, and received the master of engineering in instrumentation and controlling from the Institute of Technology of Bandung, Indonesia in 1999. He is currently working as a researcher in National Research and Innovation Agency, specified for studying renewable energy including photovoltaic power plants; wind energy power plant; geothermal energy power plants in the Research Center for Energy Conversion and Conservation. He can be contacted at email: ario001@brin.go.id or ariowitjakso@gmail.com.



Taurista Perdana Syawitri    holds a PhD degree from the School of Engineering, University of the West of England, United Kingdom. She is currently a researcher at the Research Center for Conversion and Conservation Energy, Research Organization for Energy and Manufacture, National Research and Innovation Agency (BRIN) Republic of Indonesia. Her research areas are wind energy, computational fluid dynamics, aerodynamics, fluid mechanics, hydrogen storage and energy management. She can be contacted at email: taur003@brin.go.id.



Agustina Putri Mayasari    received a degree in mechanical engineering from the Institute of Budi Utomo, Indonesia, in 2023. Currently, she is an engineering researcher at the National Research and Innovation Agency of the Republic of Indonesia (BRIN). Her research interests encompass the applications of renewable energy. She can be contacted via email at agus133@brin.go.id.